JACS
JOURNAL OF THE AMERICAN CHEMICAL SOCIETY

Subscriber access provided by ISTANBUL TEKNIK UNIV

Article

Early Homogenous Amorphous Precursor Stages of Calcium Carbonate and Subsequent Crystal Growth in Levitated Droplets

Stephan E. Wolf, Jork Leiterer, Michael Kappl, Franziska Emmerling, and Wolfgang Tremel

J. Am. Chem. Soc., **2008**, 130 (37), 12342-12347 • DOI: 10.1021/ja800984y • Publication Date (Web): 22 August 2008

Downloaded from http://pubs.acs.org on February 8, 2009

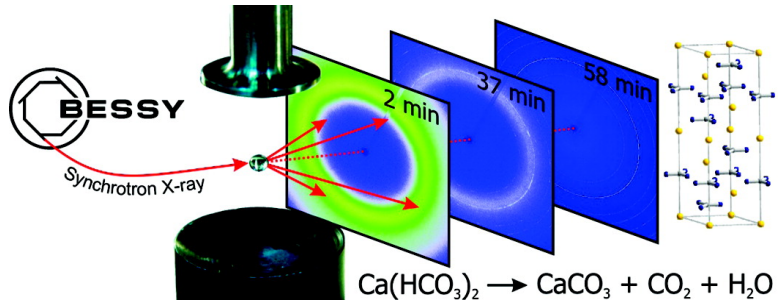

More About This Article

Additional resources and features associated with this article are available within the HTML version:

- Supporting Information
- Links to the 1 articles that cite this article, as of the time of this article download
- Access to high resolution figures
- Links to articles and content related to this article
- Copyright permission to reproduce figures and/or text from this article

View the Full Text HTML

ACS Publications
High quality. High impact.

Journal of the American Chemical Society is published by the American Chemical Society. 1155 Sixteenth Street N.W., Washington, DC 20036

J|A|C|S
ARTICLES

Published on Web 08/22/2008

Early Homogenous Amorphous Precursor Stages of Calcium Carbonate and Subsequent Crystal Growth in Levitated Droplets

Stephan E. Wolf,[†] Jork Leiterer,[‡] Michael Kappl,[§] Franziska Emmerling,[‡,*] and Wolfgang Tremel[†,*]

Institute for Inorganic Chemistry, Johannes Gutenberg-University, Duesbergweg 10-14, D-55099 Mainz, Germany, BAM Federal Institute of Materials Research and Testing, Richard-Willstätter-Strasse 11, D-12489 Berlin, Germany, and Max-Planck-Institute for Polymer Research, Ackermannweg 10, D-55128 Mainz, Germany

Received February 7, 2008; E-mail: franziska.emmerling@bam.de; tremel@uni-mainz.de

Abstract: An *in situ* study of the contact-free crystallization of calcium carbonate in acoustic levitated droplets is reported. The levitated droplet technique allows an *in situ* monitoring of the crystallization while avoiding any foreign phase boundaries that may influence the precipitation process by heterogeneous nucleation. The diffusion-controlled precipitation of $CaCO_3$ at neutral pH starts in the initial step with the homogeneous formation of a stable, nanosized liquid-like amorphous calcium carbonate phase that undergoes in a subsequent step a solution-assisted transformation to calcite. Cryogenic scanning electron microscopy studies indicate that precipitation is not induced at the solution/air interface. Our findings demonstrate that a liquid−liquid phase separation occurs at the outset of the precipitation under diffusion-controlled conditions (typical for biomineral formation) with a slow increase of the supersaturation at neutral pH.

Introduction

The formation of calcium carbonate has been studied for more than a century with more than 3000 papers over the past 10 years. Whereas the undesired precipitation of calcium carbonate is a persistent, expensive, and widespread problem,[1] the directed formation of calcium carbonate with controlled particle size, shape, and crystallographic phase is crucial for various commercial applications.[2] Crystallization of calcium carbonate in natural environments may be summarized under the label biomineralization.[3] Examples are the formation of seashells, bone, teeth, etc. This includes processes where precipitation occurs in the presence of large organic molecules resulting in the formation of hierarchically ordered inorganic−organic hybrid structures. Recently, much attention has been devoted to amorphous calcium carbonate (ACC) as a singular material, because there is increasing evidence that this phase plays a crucial role in biomineralization. ACC is the most unstable form of calcium carbonate, and under ambient conditions, it transforms quickly into more stable crystalline forms, such as vaterite and calcite.[4] Many mineralization processes are now believed to occur through the transformation of a transient amorphous precursor,[5] which has been shown to act as a reactive in intermediate in generating complex functional materials.[6]

Various analytical methods such as fast drying,[7] cryogenic transmission electron microscopy (cryo-TEM),[8] small- and wide-angle X-ray scattering (SAXS/WAXS),[9] and X-ray microscopy[10] have been utilized to observe the initial formation steps. Rieger et al. studied the formation of calcium carbonate at high supersaturation ($c \approx 0.01$ mol/L, i.e., during precipitation) after rapid mixing of the reactants $CaCl_2$ and Na_2CO_3. Cryo-TEM studies revealed the formation of emulsion-like structures preceding the precursor stage and triggered speculations about a spinodal phase separation between a denser and a less dense phase.[7] Faatz et al. reported the formation of calcium carbonate from a reaction of calcium chloride with carbon dioxide, which was homogeneously released to the solution through the alkaline hydrolysis of alkyl carbonate. Here the homogeneous formation

[†] Johannes Gutenberg University of Mainz.
[‡] BAM Federal Institute of Materials Research and Testing.
[§] Max-Planck-Institute for Polymer Research.

(1) (a) Ramstad, K.; Tydal, T.; Askvik, K. M.; Fotland, P. In *6th International Symposium on Oilfield Scale*, SPE 87430; Aberdeen: U.K., 2004. (b) Zhang, Y. P.; Shaw, H.; Farquhar, R.; Dawe, R. *J. Pet. Sci. Eng.* **2001**, *29* (2), 85–95. (c) Rieger, J.; Hadicke, E.; Rau, I. U.; Boeckh, D. *Tens. Surf. Det.* **1997**, *34* (6), 430–435. (d) Kind, M. *Chem. Eng. Process* **1999**, *38* (4−6), 405–410.
(2) Gill, R. A. PCC Fillers: High Opacity and a Whole Lot More. In *TAPPI: 1990*; Wu, K.-T., Ed.; Int. Pat. PCT/US 1996/016606.
(3) (a) Lowenstam, H. A.; Weiner, S., *On Biomineralization*. University Press: Oxford, 1989; (b) Bäuerlein, E., *Biomineralization*. Wiley-VCH: Weinheim, 2004.
(4) (a) Meldrum, F. C. *Int. Mater. Rev.* **2003**, *48*, 187. (b) Addadi, L.; Raz, S.; Weiner, S. *Adv. Mater.* **2003**, *15*, 959.
(5) Beniash, E.; Addadi, L.; Weiner, S. *J. Struct. Biol.* **1999**, *125* (1), 50–65.
(6) (a) Gehrke, N.; Nassif, N.; Pinna, N.; Antonietti, M.; Gupta, H. S.; Cölfen, H. *Chem. Mater.* **2005**, *17*, 6514. (b) Cheng, X. G.; Gower, L. B. *Biotechnol. Prog.* **2006**, *22*, 141.
(7) Cölfen, H.; Qi, L. M. *Chem.−Eur. J.* **2001**, *7* (1), 106–116.
(8) Rieger, J.; Frechen, T.; Cox, G.; Heckmann, W.; Schmidt, C.; Thieme, J. *Faraday Discuss.* **2007**, *136*, 265–277.
(9) (a) Bolze, J.; Peng, B.; Dingenouts, N.; Panine, P.; Narayanan, T.; Ballauff, M. *Langmuir* **2002**, *18* (22), 8364–8369. (b) Pontoni, D.; Bolze, J.; Dingenouts, N.; Narayanan, T.; Ballauff, M. *J. Phys. Chem. B* **2003**, *107* (22), 5123–5125. (c) Chen, T.; Neville, A.; Sorbie, K.; Zhong, Z. *Faraday Discuss.* **2007**, *136*, 355–365.
(10) Rieger, J.; Thieme, J.; Schmidt, C. *Langmuir* **2000**, *16* (22), 8300–8305.

 10.1021/ja800984y CCC: $40.75 **© 2008 American Chemical Society**

of CO_2 in the reaction medium prevents the formation of a gas−liquid interface and the formation of amorphous calcium carbonate is postulated to proceed by a liquid−liquid binodal phase separation mechanism,[11,12] but no analytical support for the formation of the proposed emulsion-like early stages could be provided. Navrotsky explains the formation of monodisperse nanoparticles within the classical (LaMer) nucleation and growth model.[13]

The main disadvantage of most experimental approaches to the precipitation of calcium carbonate lies in the diverse and poorly defined precipitation conditions. First, by way of the heterogeneous dissociation equilibrium of carbonic acid, the pH plays an important role. Furthermore, in most studies, solutions of the precursors were rapidly mixed under turbulent conditions in order to achieve a sufficiently large supersaturation. There are severe disadvantages of the rapid mixing approach. The system starts reacting at the interface of two intermixing liquid educts, but a state of homogeneous supersaturation is not reached.[14] As a result, artifacts can occur, for example, by assuming an instantaneous reaction at the interfaces of the two reactants that meet in the mixing device.[15] From this preliminary state, primary particles form with sizes in the nanometer range.

The emergence of a new phase within a mother phase is one of the most fundamental aspects of phase transitions in general and of crystal growth in particular. Furthermore, it is strongly affected by foreign bodies (e.g., macromolecules, spectator ions, liquid/liquid- or solid/liquid-interfaces, e.g., from vessel walls or due to mixing processes).[16] The potential barrier of homogeneous nucleation, which must be overcome for the formation of a new phase, is a function of the interfacial energy between the crystal and the mother phase. Therefore, foreign materials and their phase boundaries will have an impact not only on the nucleation and crystal growth rates but also on the particle size distribution of the product. They can induce a shift away from a homogeneous nucleation mechanism by energetically favoring a heterogeneous path. As a result, it is very difficult to study homogeneous nucleation respective phase separation without intervening heterogeneous bodies, for example, walls of a nozzle or a mixing chamber. It is therefore still a matter of controversy, whether genuine homogeneous nucleation can be observed at all, as it is almost impossible to remove any foreign body or phase boundary from a system.

Acoustic levitation permits a *contact-free* crystallization with a minimum of perturbations and requirements for the levitated liquid samples,[17] and it can be monitored *in situ* using synchrotron X-ray scattering techniques. The solution/air interface is the only remaining phase boundary; no other contact or foreign materials are present.

An acoustic levitator allows a contactless sample positioning and eliminates the influence of the solid container wall. In addition, *in situ*-monitoring of solutions and suspensions during evaporation of the solvent is possible for 3 orders of magnitude in concentration. In a levitated droplet, the analyte mass is constant during evaporation and no losses occur. This is an advantage over cuvettes, where sorption processes on the walls have to be considered. Working at an oscillating frequency of 58 kHz, a piezoelectric vibrator acts as an ultrasonic radiator (see Figure 1).[18] A standing acoustic wave is generated between this sonotrode and a concentrically adjusted reflector at a distance of some multiple of half the wavelengths. In several sound pressure nodes of this wave, as a result of axial radiation pressure and radial Bernoulli stress, liquid and solid samples can be placed and held in a levitated position without contact. Typically, levitated samples have a volume of 5 nL−5 μL (corresponding to a diameter of 0.2−2 mm). No other constraints on the sample such as magnetic or dielectric properties apply for acoustic levitation.

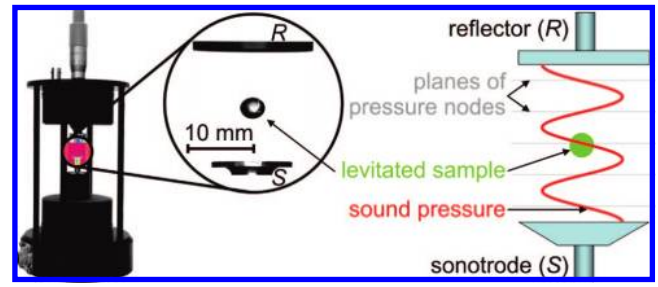

Figure 1. Photograph (left) and mode of operation (right) of the acoustic levitator. A droplet of water is levitated in the central node of the standing acoustic wave (inset) between the sonotrode *S* and a concentrically adjusted reflector *R* to demonstrate the levitation of a liquid sample.

Apart from the ultrasonic levitation method applied here, only a few other methods are applicable for an *in situ* monitoring of crystallization and phase transition processes under contact-free conditions, but either special requirements have to be met or the methods are not *contact-free* in a strict sense. Electromagnetic levitation requires electrical conductivity of the samples,[19] whereas methods based on electrostatic levitation operate under vacuum.[20] Free-jet methods require a fast mixing of educts before generating a steady-state jet of the intermixed liquids through a nozzle; the intermediates are captured by cryo-TEM.[21] This combination of methods implicates various artifacts: (i) The mixing may be incomplete due to turbulent conditions as discussed above.[15] (ii) The precipitation is not contact-free and suffers from walls contacts of the mixing chamber. (iii) Rieger et al. stated some uncertainties in sample preparation for cryo-TEM, such as differences in (local) cooling rates.[21]

This work reports a time-resolved investigation of the contact-free homogeneous formation and growth of calcium carbonate in levitated droplets studied from undersaturated to supersaturated concentrations in a single experiment. The crystallization was monitored by *in situ* WAXS experiments performed at a synchrotron microspot beamline equipped with an ultrasonic levitator. In addition, different stages of the crystallization were characterized by transmission electron microscopy as well as

(11) Faatz, M.; Gröhn, F.; Wegner, G. *Adv. Mater.* **2004**, *16* (12), 996–1000.
(12) Faatz, M. Dissertation. Johannes Gutenberg-Universität, Mainz, 2005.
(13) (a) LaMer, V. K.; Dinegar, R. H. *J. Am. Chem. Soc.* **1950**, *72* (11), 4847–4854. (b) Navrotsky, A. *Proc. Natl. Acad. Sci. U.S.A.* **2004**, *101* (33), 12096–12101.
(14) Horn, D.; Rieger, J. *Angew. Chem., Int. Ed.* **2001**, *40*, 4330–4361.
(15) Haberkorn, H.; Franke, D.; Frechen, T.; Goesele, W.; Rieger, J. *J. Colloid Interface Sci.* **2003**, *259*, 112–126.
(16) Pimpinelli, A.; Villain, J. *Physics of Crystal Growth*; University Press: Cambridge, 1998.
(17) Leiterer, J.; Leitenberger, W.; Emmerling, F.; Thünemann, A. F.; Panne, U. *J. Appl. Crystallogr.* **2006**, *39*, 771–773.
(18) (a) Lierke, E. G. *Acustica* **1996**, *82* (2), 220–237. (b) Santesson, S.; Nilsson, S. *Anal. Bioanal. Chem.* **2004**, *378* (7), 1704–1709.
(19) (a) Herlach, D. M. *Annu. Rev. Mater. Sci.* **1991**, *21*, 23–44. (b) Herlach, D. M.; Cochrane, R. F.; Egry, I.; Fecht, H. J.; Greer, A. L. *Int. Mater. Rev.* **1993**, *38* (6), 273–347.
(20) (a) Kelton, K. F.; Lee, G. W.; Gangopadhyay, A. K.; Hyers, R. W.; Rathz, T. J.; Rogers, J. R.; Robinson, M. B.; Robinson, D. S. *Phys. Rev. Lett.* **2003**, *90* (19), 195504.
(21) Haberkorn, H.; Franke, D.; Frechen, T.; Goesele, W.; Rieger, J. *J. Colloid Interface Sci.* **2003**, *259* (1), 112–126.

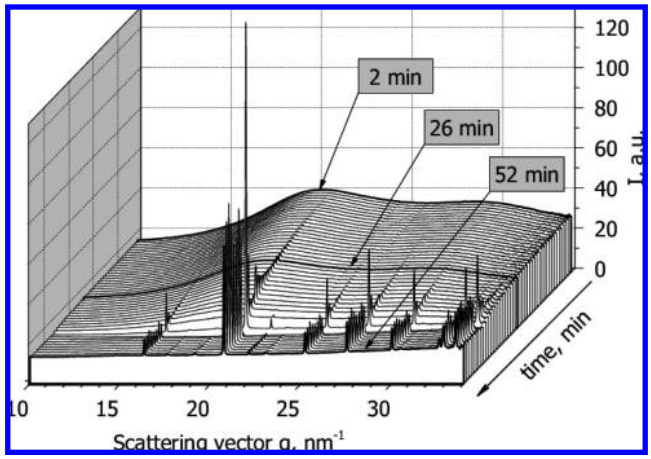

Figure 2. Scattering curves during a 1 h of evaporation experiment where each diffraction pattern was recorded with an exposure time of 40 s.

by cryogenic and standard scanning electron microscopy (cryo-SEM and SEM).

Results and Discussion

Results. *In Situ* WAXS Experiments. A droplet of an aqueous solution of calcium bicarbonate with a volume of about 4 μL was injected in an ultrasonic levitator. The calcium bicarbonate concentration increases due to the evaporation of water, and calcium carbonate starts precipitating due to the release of carbon dioxide. Starting from subcritical concentrations regarding precipitation and supersaturation, turbulent mixing conditions of the educts are strictly avoided, and the influence of foreign phase boundaries except for the air/solution-interface (e.g., vessel walls during preparation or injection into the levitator) can be ruled out.

The mineralization was monitored by time-resolved WAXS. The respective diffraction patterns are presented in Figure 2. The first patterns show only the diffuse scattering of water, which vanishes gradually as the water evaporates. The first detectable reflection belongs to the (104) set of the calcite lattice planes; its intensity increases throughout the experiment. Other calcite reflections (102), (110), (113), and (202) are detectable after 22 min, whereas the weak (006) reflection was observed after 34 min. The absence of a preferred orientation of the calcite crystals can be deduced from the spot-free and continuous Debye−Scherrer rings in the 2D frames (see Figure 3 left). A minimum of the mean particle diameter can be estimated to approximately 110 nm from the Scherrer equation based on the (012) reflection at lowest q.[22] These values are in line with particle diameters obtained from TEM and cryo-SEM (*vide infra*).[23] *In situ* WAXS experiments do not indicate the presence of crystalline phases other than calcite in significant amounts; traces of vaterite were observed only in the final stages of the droplet evaporation (<5% based on the results of Rietveld refinements).[24]

Characterization of Early Amorphous Stages. The first particles formed during the early stages of the experiment and imaged by a microscope (Figure 3) consist mainly of amorphous calcium carbonate as confirmed by the absence of Bragg diffraction peaks in the XRD patterns. These nanospheres give rise to an opalescent appearance of the droplets due to particle agglomeration (Figure 3, right).

These early amorphous reaction stages were characterized by TEM. The primary product consists of nanospheres with an emulsion-like appearance (Figure 4a, b). These particles do not form at the droplet surface as no particle formation was observed in samples taken after 400 s from the surface of a bulk solution of calcium bicarbonate by a Langmuir-Schäfer transfer. The low contrast variation within the particles indicates their liquid-like character. Solid spherical particles would show a distinct increase in contrast from the surface to the center of the particles. Particle diameters range from 100 to 300 nm, and their amorphous state was confirmed by electron diffraction (ED, see inset in Figure 4b). Remarkably, these amorphous particles are stable without stabilizing surfactants for several hours up to a few days. After long storage or upon radiation damage, crystallization commences. If articial nuclei (e.g., gold nanoparticles) are present, particles with a very different, nonliquid appearance were formed (see Experimental Section and Figures S5 and S6 in the Supporting Information).

Phase Transformation from Amorphous Calcium Carbonate to Calcite. During the early stages of the crystallization, all Bragg reflections appear split. As an example the (104) reflection profile at $q = 20.68$ and 20.79 nm^{-1} is shown in Figure S1 (Supporting Information). This "doubling" of reflections is caused by diffraction from two separate areas of the levitated droplet due to differences in the distance between detector and sample. The distance can be calculated as 1.52 mm, according to the geometrical relations given in Figure S2 (Supporting Information). This finding shows that the phase transformation process from amorphous calcium carbonate to crystalline calcite starts at the droplet surface and thus clearly differs from the crystallization within the droplets.[17]

To determine, whether the amorphous particles initially form heterogeneously at the air/water-surface or homogenously in solution, a droplet was vitrificated in liquid ethane, fractured, and the frozen droplet fragments were dried slowly by ice sublimation. Cryo-SEM revealed that these first particles form homogenously within the droplet volume (Figure 5). The particle diameter is in perfect agreement to those determined by TEM. When a droplet was levitated for about 400 s, a 20 μm thick layer was formed at the droplet surface. The particle density in this surface layer is much higher than particle number density within the volume of the droplet. As the droplet shrinks due to solvent evaporation, the particles accumulate close to the droplet surface. The sharp inner boundary without any gradient of the particle density clearly indicates that the particles are only collected and not formed within the surface layer. This effect may be viewed as a three-dimensional variant of the so-called "coffee-stain effect".[25]

(22) Klug, H. P.; Alexander, L. E. *X-Ray Diffraction Procedures: For Polycrystalline and Amorphous Materials*, 2nd ed.; Wiley-Interscience: New York, 1974; p 992.

(23) For higher scattering vectors the integral width of the reflections increases monotonically resulting in an apparent smaller calculated size of the crystallites (see Supporting Information concerning the Scherrer equation for further details). The advantage of a determination of particle diameters using the Scherrer method lies in the possibility to obtain average values for large quantities, whereas particle sizes determined by TEM or SEM are (ideally) average values for a small number (approx. 50) of particles. See Borchert, H.; Shevehenko, E. V.; Robert, A.; Mekis, I.; Kornowski, A.; Grubel, G.; Weller, H. *Langmuir* **2005**, *21* (5), 1931–1936.

(24) Rietveld, H. M. *J. Appl. Crystallogr.* **1969**, *2*, 65–71.

(25) (a) Deegan, R. D.; Bakajin, O. F.; Dupont, T.; Huber, G.; Nagel, S. R. A.; Witten, T. *Nature* **1997**, *389*, 827–830. (b) Loges, N.; Therese, H. A.; Graf, K.; Nasdala, L.; Tremel, W. *Langmuir* **2006**, *22*, 3073–3080.

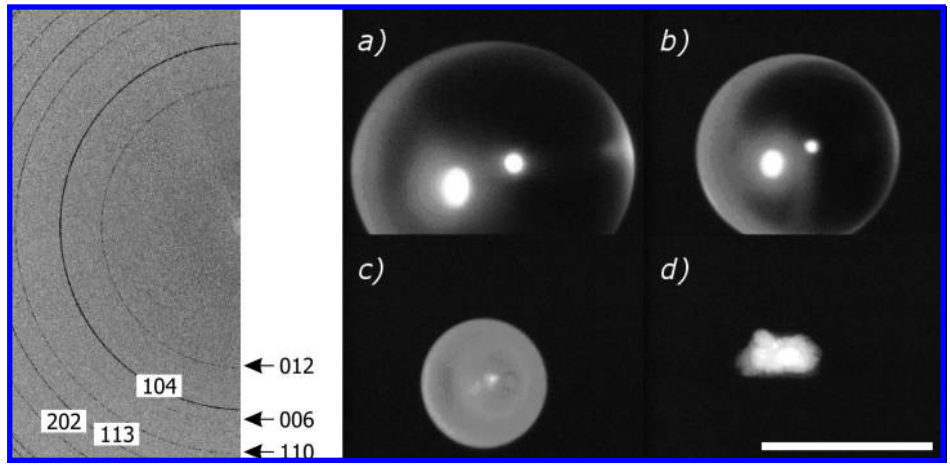

Figure 3. Representative 2D detector frame, measured in a late state of the experiment (left). Microscopy images of the evaporation of a solution of $Ca(HCO_3)_2$ during levitation (right). The whole droplet appears increasingly opalescent due to an aggregation of nanoparticles (a−c). The very bright spot close to the center of the droplet in (a) and (b) are due to reflected light. The last image shows the final dry residue (d). Photographs were taken after (a) 27 min, (b) 35 min, (c) 41 min, and (d) 60 min of flight. Scale bar: 1 mm.

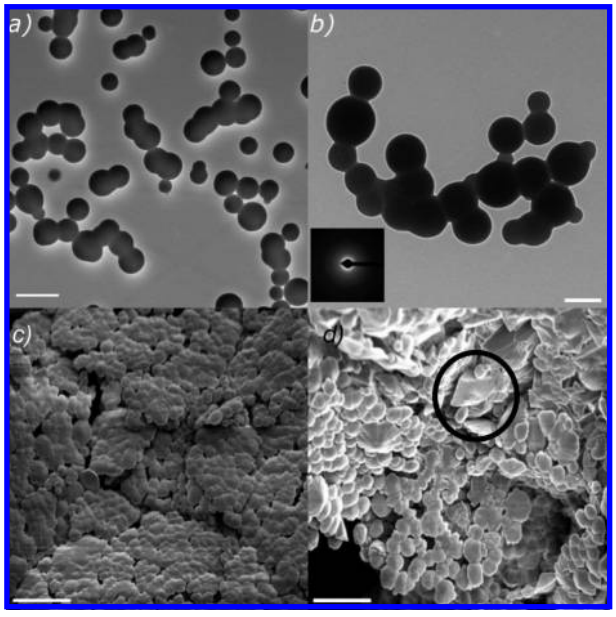

Figure 4. Calcium carbonate particles obtained after 400 s (TEM: a, b). The low contrast variation within the particles indicates their liquid character. After complete evaporation, SEM revealed that spherical solid particles are present along with rhombohedral calcite crystals (c, d). Scale bars: (a) 500 nm, (b) 200 nm, (c) 20 μm, and (d) 10 μm. On the basis of the morphology of the calcite particles, the transition to the crystalline phase is assumed to take place through recrystallization. One rhomboidal calcite crystal is marked by a circle in (d).

Scale factors s can be extracted from a Rietveld analysis of the X-ray powder data series,[22] which represent the transformed volume fraction $f_v(t)$ of the calcite phase when all the calcite scale factors are rescaled to run between zero and unity. A nonlinear least-squares fit of this evolution to the Avrami form $f_v(t) = 1 - e^{-[k_A(t-t_0)]}$ yields a value for the Avrami exponent n that mainly characterizes the kinetics of the phase formation.[26,27] For polymorphic transitions, $n \approx 3$ indicates a mechanism where nucleation occurs only at the start of a transformation, a value $n \approx 4$ indicates that the phase transformation continues to form new growing nuclei in untransformed material. Using the calcite structure as the basis for the refinement, a nonlinear least-squares fit to the Avrami form in the present case phase yields a value for the exponent $n = 8.3$, with $t_0 = 26$ min as the time, when crystallization is first seen as a Bragg reflection (c.f. plot in Figure S4, Supporting Information). This large value of $n = 8.3$ seems to indicate that the transformation rate to calcite is high, and it implies a secondary nucleation on amorphous calcium carbonate particles independent of the calcite crystallites that already exist. Thus, the observed precipitation of calcite occurs rapidly once a critical level has been reached after approximately 26 min.

The analysis of the dry residue by scanning electron microscopy (SEM) showed spherical particles with diameters of about 5 μm, together with several crystals exhibiting the rhombohedral morphology of calcite crystals (Figure 4c and d). The observed spherical particles are assumed to be solidified dry amorphous calcium carbonate, which did not transform into crystalline material.

Discussion

The supersaturation of $CaCO_3$ increases due to the loss of water by evaporation and a concomitant loss of carbon dioxide from the droplet. The primary particles are amorphous and of homogeneous origin. TEM and cryo-SEM data strongly support that the particle formation is not induced heterogeneously at the air/water interface. The calcium carbonate particles possess an emulsion-like structure, and their occurrence is compatible with a homogeneous liquid−liquid phase separation process. Upon aging, the particles continuously lose water and solidify, and amorphous calcium carbonate particles accumulate close to the surface due to shrinking of the droplet. This thin layer of particles gives rise to the opalescent appearance of the droplet.

The fact that no other calcium carbonate phase (e.g., vaterite and aragonite) or the less common phases ikaite or calcium carbonate hexahydrate appear seems to contradict Ostwald's rule of stages,[28] which states that the next phase to appear will always be the nearest state in energy. Our findings, however, can be

(26) West, A. R. *Solid State Chemistry and its Applications*; John Wiley & Sons: Chichester, 1984.

(27) (a) Avrami, M. *J. Chem. Phys.* **1939**, *7*, 1103–1112. (b) Avrami, M. *J. Chem. Phys.* **1940**, *8*, 212–224. (c) Avrami, M. *J. Chem. Phys.* **1941**, *9*, 177–184. (d) Bartz, M.; Küther, J.; Vaughan, G. B. M.; Seshadri, R.; Tremel, W. *J. Mater. Chem.* **2001**, *11*, 503–506.

(28) Ostwald, W. *Z. Phys. Chem.* **1897**, *22*, 289–330.

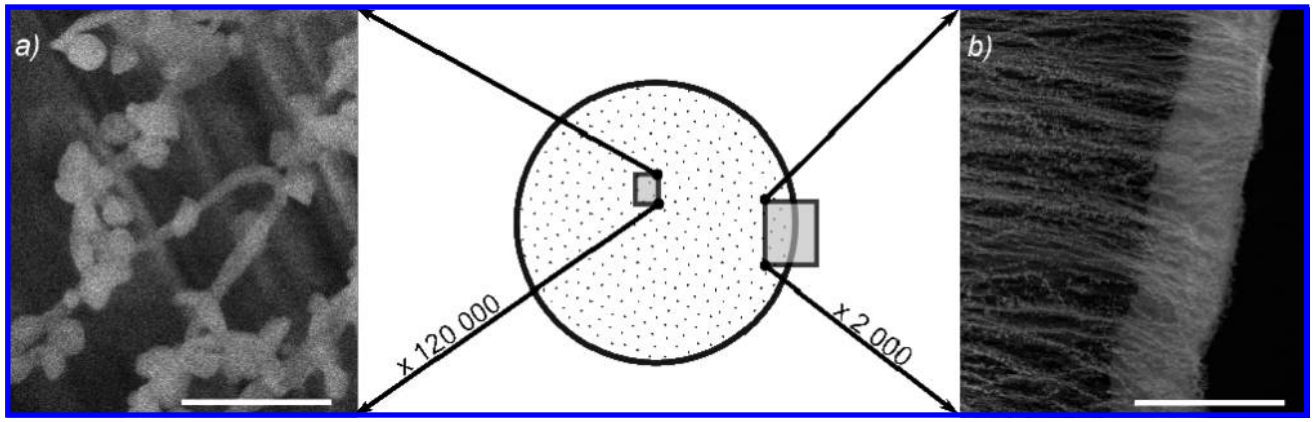

Figure 5. Cryo-SEM studies of a droplet levitated for 400 s, which was vitrificated in liquid ethane, then cryo-fractured and lyophilized. Particles form in the whole droplet volume. Their diameter is in good agreement with diameters derived from TEM studies. (a) Particles found in the inner part of the droplet are likely to be formed homogenously. (b) A 20 μm thick layer near the droplet surface develops because particles accumulate close to the surface while the droplet shrinks by evaporation. The fibrous structures in both images are artifacts due to ice devitrification. Scale bars: (a) 500 nm, (b) 40 μm.

rationalized by a templated nucleation of calcite on the surface of the amorphous precursor.[29] The accumulation of amorphous particles in the thin surface layer near the droplet surface provides a large surface area for secondary heterogeneous nucleation. The incipient calcite formation leads to the observed peak splitting in the early stages of crystallization (*vide supra* and Figure S1, Supporting Information).

Calcite formation increases rapidly after approximately 26 min. The high nucleation rate deduced from the Avrami plot is in agreement with a heterogeneous nucleation of calcite, the crystallographically detectable phase, as well. A dissolution-assisted route seems feasible due the well-developed shape of the calcite crystals. The amorphous calcium carbonate does not transform completely into calcite.

For the formation of calcium carbonate, a binodal liquid−liquid phase separation process was proposed by Faatz et al., but no analytical evidence was given.[11] Rieger et al. reported the formation of emulsion-like particles from rapid mixing at high supersaturation. In this work, we demonstrate for the first time by a combination (X-ray, TEM, cryo-SEM) of methods that a liquid−liquid phase separation of calcium carbonate does not only occur for large supersaturations in the case of a fast mixing processes at high pH, but also for a diffusion-controlled precipitation involving a slow increase of supersaturation at neutral pH. These conditions are close to the formation conditions of biominerals. The homogeneous approach, based on the Kitano-Method *without* mixing of educts,[30] does not suffer from potential artifacts due to incomplete intermixing of the precursors.

Formation of calcium carbonate by a liquid precursor has been previously observed by Gower et al.[31] This polymer-induced liquid-precursor (PILP) process is believed to play an important role in the morphogenesis of biominerals and biomimetic materials. Small amounts of small poly anionic polymers (such as polyaspartate)[31] or proteins (e.g., ovalbumin)[32] are thought to induce a liquid−liquid phase separation during crystallization and small colloidal droplets of a metastable amorphous liquid-phase mineral precursor are formed. The results reported here show that an amorphous liquid-phase mineral precursor is even formed in the absence of stabilizing polymers or additives, that is, it seems to be a characteristic feature of the homogeneous formation of calcium carbonate itself, independent of the initial supersaturation. Polymers and proteins can aid in stabilizing this liquid state, but the liquid homogeneous particles are remarkably stable at neutral pH as well.

The formation and the stability of the liquid-like phase may be rationalized by the presence of several species involved in the process. The pH value exerts not only a strong influence on the supersaturation level by controlling the concentrations of carbonate, bicarbonate, and nondissociated carbonic acid, it determines also the concentration of the active Ca^{2+} solution species that is involved in complexation and precipitation equilibria. Their hydroxyl groups can set up an extensive hydrogen-bonding network between the three carbonate species and water, which may interact with the hydrated or hydrogen carbonate-coordinated Ca^{2+} ion. Therefore, at neutral pH, this network formation of several species may favor the formation of an amorphous solid (similar as in glass forming materials such as borates) over the formation an ionic $CaCO_3$ lattice. The presence of (i) various bonding partners, (ii) variable coordination geometries and coordination numbers of the carbonate groups, and (iii) the associated distribution of local structures may favor the formation of the noncrystalline phase.

Summary and Conclusion

The first *in situ* X-ray study of the *contact-free* homogeneous precipitation of calcium carbonate in a levitated droplet has been carried out. The homogeneous formation of $CaCO_3$ proceeds via an amorphous liquid-like state. This amorphous phase formed in the absence of any stabilizing polymers or additives at neutral pH. Its stability may be related to the presence of various species such as carbonate, bicarbonate, and nondissociated carbonic acid involved in the process. The formation of an amorphous liquid-phase mineral precursor seems to be a characteristic of the truly homogeneous formation of calcium carbonate itself. These resulting primary particles serve in a second step as templates for the crystallization of calcite. Finally, $CaCO_3$ may be regarded as the first example where a liquid amorphous precursor could be identified for an inorganic mineral phase unambiguously without artifacts.[15]

(29) Shen, Q.; Wei, H.; Zhou, Y.; Huang, Y.; Yang, H.; Wang, D.; Xu, D. *J. Phys. Chem. B* **2006**, *110*, 2994–3000.
(30) (a) Kitano, Y. *Bull. Chem. Soc. Jpn.* **1962**, *35* (12), 1973–1980. (b) Kitano, Y. *Bull. Chem. Soc. Jpn.* **1962**, *35* (12), 1980–1985.
(31) Gower, L. B.; Odom, D. J. *J. Cryst. Growth* **2000**, *210* (4), 719–734.
(32) Pipich, V.; Balz, M.; Wolf, S. E.; Tremel, W.; Schwahn, D. *J. Am. Chem. Soc.* **2008**, *130*, 6879.

Our results show the ultrasonic trap to be a powerful tool for a real-time analysis of nucleation, crystal growth, and phase separation processes by reducing disturbances and artifacts due to solid phase boundaries to a minimum. Thus, acoustic levitation provides a reliable sample environment for studies of homogeneous precipitation reactions.

Experimental Section

The crystallization was carried out homogenously according to the Kitano method.[30] By slow evaporation of water or a slow release of carbon dioxide from a saturated solution of calcium bicarbonate, calcium carbonate is formed.

$$Ca(HCO_3)_2 \rightarrow CaCO_3 + CO_2 + H_2O$$

Carbon dioxide (Westfalen AG) was bubbled through 20 mL of a suspension of $CaCO_3$ (p. a., Sigma Aldrich) in ultra pure water (Millipore Synergy 185 with UV photo oxidation, 18.2 MΩ/cm). The obtained saturated solution of calcium bicarbonate was filtered with a cascade of syringe filters, which consists of a 0.1 μm Millipore Millex VV followed by 20 nm Milipore Anotop in series. Afterward, the filtered solution was treated again extensively with carbon dioxide to dissolve nuclei with diameters < 20 nm. In control experiments, crystallization nuclei were prepared by skipping this removal step to preserve $CaCO_3$ nuclei or by adding gold nanoparticles prepared according to the method of Gittins and Caruso.[33]

One droplet of an aqueous sample with a volume of approximately 4 μL was hand-injected into the ultrasonic levitator (Tec5, Oberursel, Germany). SEM investigations were performed with a Zeiss DSM 940 running at 10 kV. Samples for cryo-SEM were prepared by plunging the respective droplet in liquid ethane and transferring it directly into a cryo-preparation chamber (FEI Quorum PolarPrep 2000), where it was cryo-fractured after removal of excessive ethane at −60 °C and 10^{-6} mbar. Under these conditions, the vitreous ice transforms into a crystalline state (which is the origin of the fibrous artifacts mentioned above). Afterward, the samples were transferred to the N_2-cooled cryo-stage of the cryo-SEM (FEI xT Nova 600 Nanolab), and the water was slowly removed by sublimation at −5 °C and 10^{-6} mbar, which was monitored *in situ* by SEM at 2−10 kV. TEM investigations were carried with a Phillips EM 420 running at 120 kV, equipped with an ORCA-ER Camera (1024 × 1024 pixel) and run with AMT Image Capture Engine v5.42.540a. The samples were prepared by transferring the respective droplet on a lacey-coated TEM grid (Plano, Germany), followed by washing with water and drying in air.

Wide-angle X-ray scattering (WAXS) experiments were performed using the μSpot beamline at BESSY (Figure 6, further information concerning the general setup are given in ref 34), which is equipped with a double crystal monochromator, yielding a monochromatic ($\lambda = 1.00257$ Å) beam. A pinhole system provides a beam of 20 μm cross section with a photon flux of about 10^9 per second and a ring current of 100 mA. The scattering pattern from

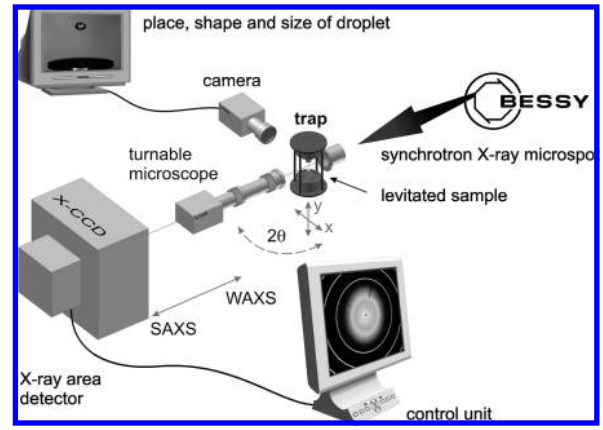

Figure 6. Experimental setup at the μSpot beamline integrates the acoustic levitator for SAXS and WAXS measurements. The levitated sample is monitored and remote controlled during the whole experiment. The pivoting microscope determines exactly the position of the 20 μm beam at the sample.

corundum serves as external calibration standard. No mathematical "desmearing" of the experimental scattering intensity function was needed due to the small beam diameter of the incident beam. In case of the levitated droplets, the scattering from the pure solvent was measured and used as an estimate of the background contribution. The data were not corrected for background scattering, as it was not possible to correlate the shrinking volume of the sample solution with that of a water droplet for every state of evaporation considering the accompanying change of X-ray absorption. The scattering vector $q = 4\pi/\lambda \sin(\theta)$ is defined in terms of the angle 2θ between incident and scattered radiation of the wavelength λ. The data were processed and converted into diagrams of scattering intensities I versus q by employing algorithms of the computer program FIT2D.[35]

Acknowledgment. We thank Simone Rolf (BAM), Maren Müller (Max-Planck-Institute for Polymer Research) for technical help, Dr. Stefan Siegel and Dr. Cheng Hao Li (Max Planck-Institute for Colloid Research) for technical support at the beam line, and Prof. Dr. A. Thünemann and Dr. Ute Kolb for helpful discussions. We are grateful to the Deutsche Forschungsgemeinschaft (DFG) for support within the priority program "Prinzipien der Biomineralisation". S.E.W. is recipient of a Konrad Adenauer-fellowship. We also acknowledge partial support from the Fonds der Chemischen Industrie.

Supporting Information Available: (1) Determination of mean crystallite size, (2) Peak splitting phenomena in early crystallization stages, (3) Avrami analysis, and (4) Crystallization in presence of foreign nuclei. This material is available free of charge via the Internet at http://pubs.acs.org.

JA800984Y

(33) (a) Schwahn, D.; Balz, M.; Bartz, M.; Fomenko, A.; Tremel, W. *J. Appl. Crystallogr.* **2003**, *36*, 583–586. (b) Gittins, D. I.; Caruso, F. *Angew. Chem., Int. Ed.* **2001**, *113*, 3089–3092.

(34) Paris, O.; Li, C. H.; Siegel, S.; Weseloh, G.; Emmerling, F.; Riesemeier, H.; Erko, A.; Fratzl, P. *J. Appl. Crystallogr.* **2007**, *40*, S466–S470.

(35) Hammersley, A. P.; Svensson, S. O.; Hanfland, M.; Fitch, A. N.; Hausermann, D. *High Press. Res.* **1996**, *14* (4−6), 235–248.